Green and Sustainable Chemistry, 2016, 6, 116-124
Published Online May 2016 in SciRes. http://www.scirp.org/journal/gsc
http://dx.doi.org/10.4236/gsc.2016.62011

CO_2 Capture at Room Temperature and Ambient Pressure: Isomer Effect in Room Temperature Ionic Liquid/Propanol Solutions

Hiroshi Abe*, Azusa Takeshita, Hirokazu Sudo, Koichi Akiyama, Hiroaki Kishimura

Department of Materials Science and Engineering, National Defense Academy, Yokosuka, Japan
Email: *ab@nda.ac.jp

Received 17 March 2016; accepted 22 May 2016; published 25 May 2016

Abstract

A CO_2 capture system without supercritical CO_2 was optimized for mixtures of hydrophobic room temperature ionic liquids (RTILs) and propanol. We tested RTILs using bis(trifluoromethanesulfonyl)imide, $TFSI^-$, anion and four quaternary ammonium cations, two quaternary phosphonium cations, and one imidazolium cation. The addition of 2-propanol into the RTILs clearly promoted the capture of normal CO_2(nCO_2) at ambient temperature and pressure. When combined with 2-propanol, the most efficient RTILs for nCO_2 capture were *N*-butyl-*N*,*N*,*N*-trimethylammonium $TFSI^-$. This enhancement of nCO_2 capture was not observed in RTIL mixtures with 1-propanol or in propanol mixtures containing other phosphonium- and imidazolium-based RTILs. The torsion angle of $TFSI^-$, which was calculated using density functional theory, is thought to be related to high nCO_2 capture efficiently.

Keywords

CO_2 Capture, Room Temperature Ionic Liquids, Propanol Isomer Effect, Torsion Angle of $TFSI^-$ Anion

1. Introduction

The emission of greenhouse gases, which warms the Earth's surface and atmosphere, is an urgent global problem. Room temperature ionic liquids (RTILs) have attracted considerable attention for the capture of carbon

*Corresponding author.

How to cite this paper: Abe, H., Takeshita, A., Sudo, H., Akiyama, K. and Kishimura, H. (2016) CO_2 Capture at Room Temperature and Ambient Pressure: Isomer Effect in Room Temperature Ionic Liquid/Propanol Solutions. *Green and Sustainable Chemistry*, **6**, 116-124. http://dx.doi.org/10.4236/gsc.2016.62011

dioxide (CO_2) in efforts to counteract global warming. The capture of CO_2 using an RTIL was first reported by physically dissolving supercritical CO_2 ($scCO_2$) at high temperature and pressure into 1-butyl-3-methylimidazolium hexafluorophosphate, [C_4mim][PF_6] [1], and the pressure-CO_2 molar fraction phase diagram was constructed at 40˚C. Since then, various theoretical [2]-[6] and experimental [7]-[13] investigations have been conducted to further develop techniques for CO_2 capture and storage in green chemistry. Systematic studies reveal that $scCO_2$ is highly soluble in the bis(trifluoromethanesulfonyl)imide ($TFSI^-$) anion-based RTIL [10] and the polymerization of RTILs has been shown to allow the reversible and fast sorption and desorption of normal CO_2 (nCO_2) [8]. To apply RTILs in actual industrial applications, developing a cost-effective system that does not require high temperature or pressure for nCO_2 capture remains necessary.

As additive effect, isomer effects of alcohols in the RTILs were observed distinctly [14]-[17]. A previous study estimated the molecular interactions between RTILs and propanol on desorption time measured under vacuum [14]. The results indicated that 1-propanol interacts more strongly with RTILs than does 2-propanol. In addition, Raman spectroscopy revealed that the propanol isomer effect is related to the conformations of $TFSI^-$ anion, which can exist as two stable conformers, *cis* (C_1) and *trans* (C_2) [18] [19]. C_1 and C_2 conformers of $TFSI^-$ originate from the competition between the alkyl side-chain length of the $C_n mim^+$ cation and the propanol isomer effect. Recently, butanol isomer effect was reported in [$C_n$mim][TFSI]-based systems with four types of butanol [17], owing to the different hydrophobicities of four types of butanol. The upper critical solution temperatures (UCSTs) in the phase diagrams were clearly separated with increasing alkyl side-chain length of the $C_n mim^+$ cation.

Systematic CO_2 solubility experiments have demonstrated that $TFSI^-$ exhibits good CO_2 capture ability in pure RTILs systems [20]. Isomer effects have been observed in $TFSI^-$-based RTILs, including [$C_n$mim][TFSI] ($2 \leq n \leq 10$) [15]. The established binary phase diagrams and UNIQUAC (universal quasichemical) interaction parameters indicate that the interactions of 1-propanol with RTILs differ significantly from the interactions between 2-propanol and RTILs.

In this study, we optimized physical sorption of nCO_2 at room temperature and ambient pressure. The dilution of RTILs with 2-propanol promoted nCO_2 capture, and stabilized the liquid mixing state. The amount of captured nCO_2 was related to the torsion angle of the $TFSI^-$ anion, which was calculated by density functional theory (DFT). The propanol isomer effect and torsion angle of $TFSI^-$ anion had critical effects on the level of nCO_2 absorption in the propanol-rich region, which is desirable for decreasing the cost of carbon capture operation.

2. Materials and Methods

Hydrophobic RTILs were used in this study to prevent contamination by water from atmospheric moisture. $TFSI^-$ is commonly used as the anion in hydrophobic RTILs. In this study, we tested four quaternary ammonium cations, *i.e.*, *N*,*N*-diethyl-*N*-methyl-*N*-(2-methoxyethyl)ammonium ($DEME^+$), ethyldimethylpropylammonium, ($N1123^+$), *N*,*N*,*N*-trimethyl-*N*-propyl ammonium ($N3111^+$), *N*-trimethyl-*N*-butylammonium ($N4111^+$), *N*-tributyl-*N*-methylammonium ($N4441^+$) and methyltrioctylammonium ($N8881^+$), two quaternary phosphonium cations, *i.e.*, triethylpentylphosphonium ($P2225^+$) and tributyl methyl phosphonium ($P4441^+$), and one prototype cation, *i.e.*, 1-butyl-3-methylimidazolium ($C_4 mim^+$). All RTILs were obtained from IoLiTecCo.1-Propanol (99.5%) and 2-propanol (99.5%; Kanto Chemical Co.) were used as additives.

For CO_2 sorption, a CO_2 flowing system was assembled. A schematic of the CO_2 sorption system is illustrated in **Figure 1**. Mixtures were put into a glass-type sample bottle (30 cc).

The sample bottle was placed on a container with flowing gas. The sample container was immersed in an ethanol bath (Yamato Scientific Co., BB301) with flowing CO_2 gas (30 mL/min) for 10 min. Temperature stability was within 0.1˚C (15˚C ≤ T ≤ 30˚C). Within 5 s, the sample was moved to the electric balance (HR-202i, A & D Co.), which monitored the desorption process of nCO_2. Gas selectivity testing was conducted using O_2 and N_2 gases.

To determine the phase diagrams of the RTIL-propanol mixtures, samples were cooled from 30˚C to −50˚C using an ethanol bath (Yamato Scientific Co., BE200). By visual cloud-point determinations, accuracy of the clouding temperatures was found to be within 0.5˚C. A liquid N_2 pot was used as a supplement for further cooling. The minimum temperature (−50˚C) is limited by viscous ethanol at low temperature. The temperature was monitored by a Pt100 temperature sensor (Netsushin Co.). The cooling rate was 1.5 C/min.

The conformational stabilities of the mixtures were examined by Raman spectroscopy using a micro-Raman spectrometer (RA-07F, Seishin-Shoji) in backscattering mode equipped with a monochromator (500M, Horiba JobinYvon) and a charge-coupled device detector (Symphony, Horiba JobinYvon). Radiation at 532 nm from a

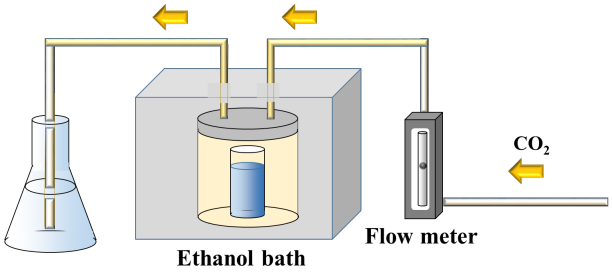

Figure 1. Schematic illustration of nCO$_2$ sorption assembly.

Nd:YAG laser (power = 50 mW) was used as the excitation source.

3. Results and Discussion

3.1. nCO$_2$ Capture in RTIL-Propanol Mixtures

Figure 2 shows the amount of captured nCO$_2$ as a function of propanol concentration in the [N4111][TFSI]-propanol system at a temperature of 25˚C. The molar fraction of nCO$_2$ was calculated as,

$$\eta = \frac{n_{CO_2}}{n_{IL} + n_{CO_2}} \times 100(\%) \tag{1}$$

where n_{IL} and n_{CO_2} are the moles of RTILs and nCO$_2$, respectively. We did not consider the amount of propanol in this study, as propanol is relatively inexpensive compared with the RTILs. The results show that the addition of 2-propanol can promote nCO$_2$ capture in the propanol-rich region. In contrast, 1-propanol did not enhance nCO$_2$ capture. The value of η for the 1-propanol-based mixtures remained almost constant with changing propanol concentration; this is a typical isomer effect of propanol, as indicated by the phase diagrams [15]. The isomer effect of nCO$_2$ capture is discussed in the next section along with liquid stability. The above tendency is also seen in other systems. The molar fractions at the points of maximum nCO$_2$ sorption for all RTILs-propanol systems studied herein are indicated in **Figure 3**. Here, temperature was fixed at 25˚C. The nCO$_2$ sorption of the 1-propanol-based mixture was larger than that of the 2-propanol one only for the [DEME][TFSI] system. Relative large values of η were obtained in the quaternary ammonium cation-based systems. In contrast, the phosphonium and imidazolium systems exhibited lower nCO$_2$ capture abilities. The high efficiency of nCO$_2$ capture in the quaternary ammonium cation-based systems can be attributed to the syntheses of these cations. An example of synthesis using the Halogen-free carbonate ester method [21] can be written as follows:

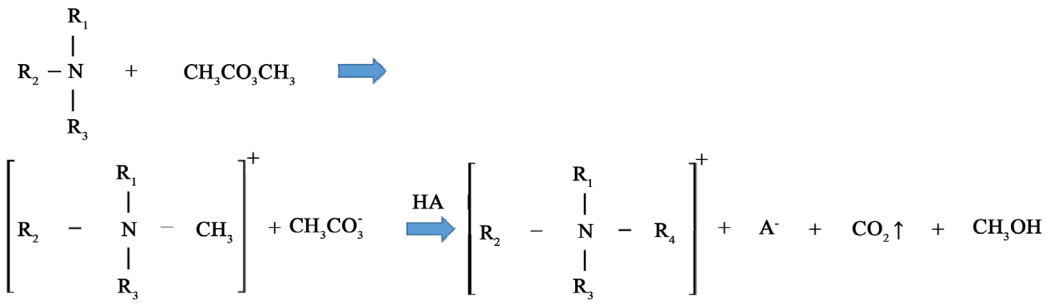

(2)

The scheme in Equation (2) leads to the coexistence of quaternary ammonium cation, alcohol and CO_2, and provides a clue to explain the high nCO$_2$ capture obtained using quaternary ammonium cations. We predict that the cation, CO_2 and alcohol are affirmative each other. Among the RTILs used in this study, the [N4111][TFSI]-2-propanol system provided the best nCO$_2$ storage.

3.2. Thermal Properties of nCO$_2$ Capture

To investigate the thermal characteristics of nCO$_2$ capture, the η value of the [N4111][TFSI]-80 mol% 2-propanol

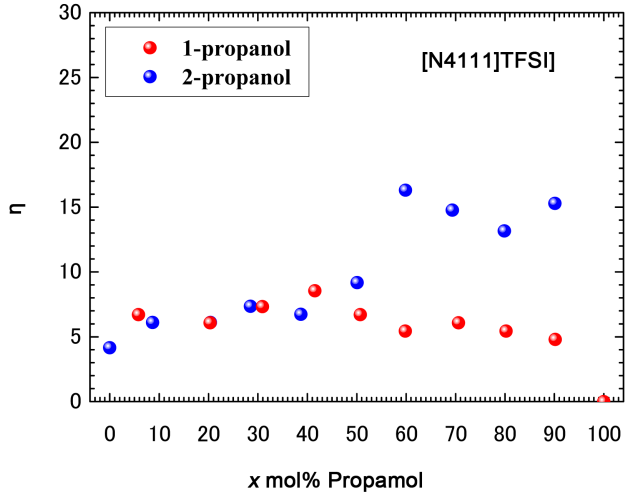

Figure 2. Dependence of nCO_2 molar fraction, η (%), on propanol concentration, showing the propanol isomer effect at 25˚C. High nCO_2 sorption is observed in the propanol-rich region.

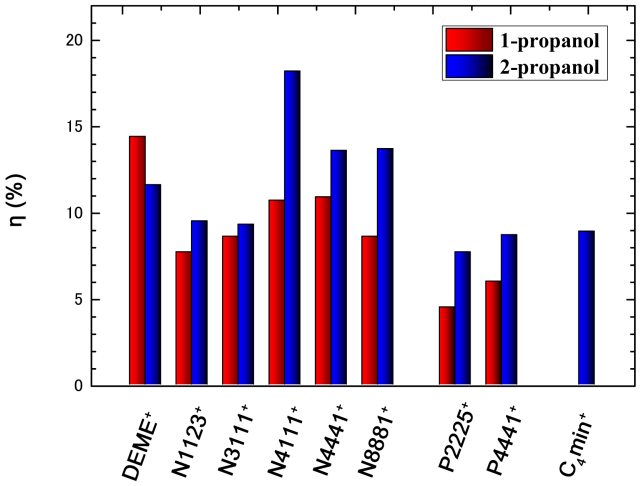

Figure 3. Maximum nCO_2 sorption in various RTILs-propanol systems. With the exception of the [DEME][TFSI]-propanol system, the 2-propanol-based mixtures have a preference for nCO_2 capture. Quaternary ammonium RTILs possess relative high abilities for nCO_2 capture.

system is plotted as a function of temperature in **Figure 4(a)**. Upon cooling down to 15˚C, almost monotonic increase of η was observed. According to conventional thermodynamics, η decreases with increasing temperature. At lower temperature, CO_2 absorption efficiency was elevated. In [N4111][TFSI]-propanol system, however, there is a problem of phase separation in the propanol-rich region. **Figure 4(b)** reveals the phase diagram of [N4111][TFSI]-1-propanol and -2-propanol. The phase diagram of [N4111][TFSI]-propanol system was constructed based on visual cloud-point determinations [14] [15] [17]. The cloud-points of 1- and 2-based mixtures are represented by red and blue closed circles, respectively. On the phase diagrams, different molecular interactions of 1- and 2-propanol was predominant, since phase separation curves are calculated using the UNIQUAC interaction parameters [15]. The UNIQUAC model has the nearest neighbor correlation. The UCST of the [N4111][TFSI]-80 mol% 2-propanol mixture was approximately 15˚C. Therefore, below 15˚C, it is impossible to use nCO_2 capture in the [N4111][TFSI]-2-propanol system for industrial applications.

Phase diagram including phase instability is connected with nCO_2 capture ability in the propanol-rich region

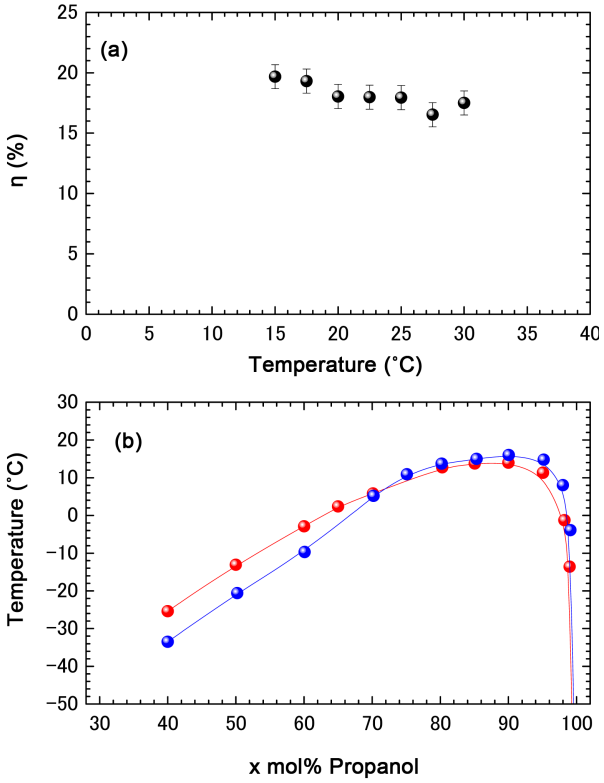

Figure 4. (a) Temperature dependence of nCO$_2$ molar fraction (η) in [N4111][TFSI]-80 mol% 2-propanol; (b) Phase diagram of the [N4111][TFSI]-propanol system.

(**Figure 2**). At the UCST, the phase separation behavior could significantly influence the nCO$_2$ capture. Generally, liquid becomes unstable as a precursor phenomenon close to phase separation. Fluctuations in the propanol concentration in the vicinity of the clouding point were not ignored. Furthermore, UCST and the critical concentration (x_c = 85 mol%) in the phase diagram have significant meaning on the UCST [15]. In thermodynamics, fluctuations are critical phenomena that are enhanced at UCST and x_c. In this study, the intrinsic instability of the liquid phase in the RTILs-propanol mixtures became distinct at around x_c. Thus, we deduce that the unstable liquid phase in the propanol-rich region was stabilized by nCO$_2$ sorption.

3.3. TFSI$^-$ Conformation and nCO$_2$ Capture

TFSI$^-$ conformation stabilities in the RTIL-propanol mixtures were estimated by Raman spectroscopy [15] [17]-[19] [22]. The observed Raman bands were assigned as C_1/C_2 conformers by DFT calculations [18] [22]. As an example, the Raman spectrum of pure [N4111][TFSI] is shown in **Figure 5(a)**. The experimental C_2/C_1 ratio was calculated by decomposing the Raman peaks, and the asymmetric pseudo-Voigt function was used to separate peaks. The highest level of nCO$_2$ capture for [N4111][TFSI] was obtained at C_2/C_1 = 0.539. In contrast to [N4111][TFSI], the C_2/C_1 values of [N1123][TFSI] and [P2225][TFSI], which exhibited poor nCO$_2$ capture abilities, were 0.853 and 0.869, respectively. For instance, the Raman spectrum of [P2225][TFSI] is displayed in **Figure 5(b)**. Despite pure systems, the C_2/C_1 ratio of TFSI$^-$ anion is regarded as a good indicator of nCO$_2$ capture ability, and C_2/C_1 has been used to determine the mixing states of [C$_n$mim][TFSI]-propanol [15] and -butanol [17]. In both the pure and mixed systems, the TFSI$^-$ anion conformer indicates energetically stable/unstable states in the liquid state.

DFT calculations are indispensable to interpret experimental results, although DFT calculations provide the molecular-level details on the gas phase. DFT calculations were performed using the Lee-Yang-Peer correlation (B3LYP) with the 6-31++G(d,p) basis set [23] [24] in the PC-GAMESS package [25]. In the DFT simulation box, we introduced the torsion angle (α) of TFSI$^-$ anion (**Figure 6(a)**); the geometrical definition of α was provided

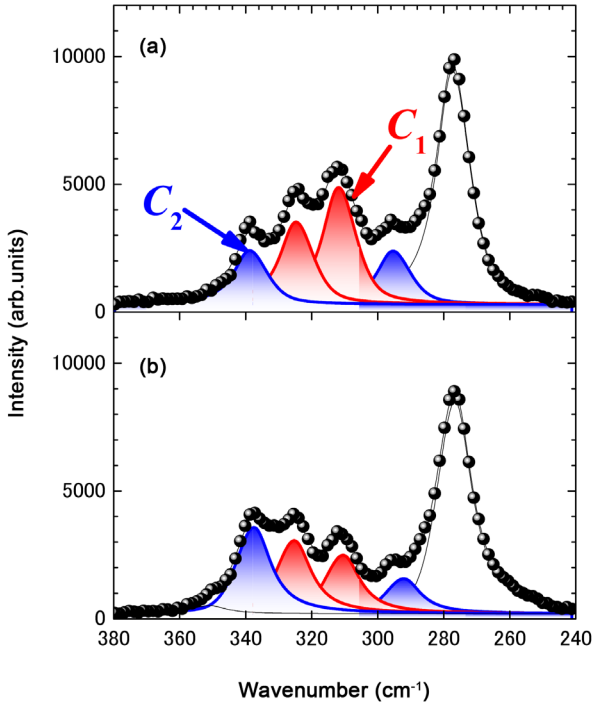

Figure 5. Raman spectrum of (a) pure [N4111][TFSI], and (b) [P2225][TFSI] at room temperature. The decomposed peaks are assigned as C_1 and C_2 conformers of $TFSI^-$.

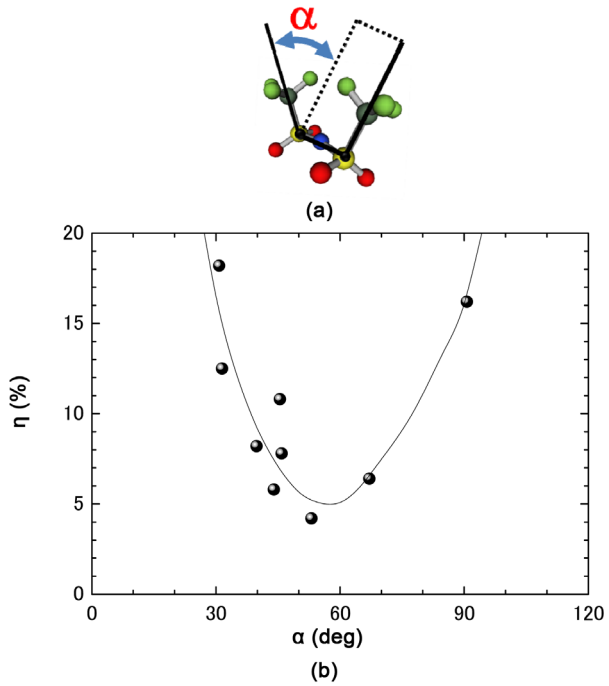

Figure 6. (a) Definition of torsional angle α, (C-S-S-C) in $TFSI^-$; (b) nCO_2 molar fraction (η) as a function of calculated torsion angle.

by the C-S-S-C angle. DFT calculations of the [N4111][TFSI] system were used to examine a relation between a of $TFSI^-$ and molecular configurations of propanol isomer and CO_2 additive (**Table 1**). The calculated torsion

angle is sensitive to the presence of propanol and its conformation. In pure [N4111][TFSI], α = 30.756˚; the addition of 2-propanol increased the torsion angle to 72.517˚. The effect of 2-propanol on torsion angle was larger than that of 1-propanol. These results are in agreement with previous DFT calculations. The experimentally obtained C_2/C_1 ratio of $TFSI^-$ anion is known to reflect the stabilities of the liquid, glass, and solid phases [14] [15] [17] [26]. Thus, increased α in the [N4111][TFSI]-2-propanol mixture has significant implications for liquid state stabilization. The torsional potential of $TFSI^-$ anion has two local minima at 80˚ and 280˚ [27]. Although the potential calculated between the two minima is relatively low, $TFSI^-$ has a higher torsional barrier at approximately 0˚ (C_1). Hence, in case of the [N4111][TFSI]-2-propanol mixture, 2-propanol causes the $TFSI^-$ anion to twist, and stabilizes energetically. In the [N4111][TFSI]-1-propanol system, α cannot reached to 70˚. The difference in α between the 1- and 2-propanol-based RTILs is directly connected to the propanol isomer effect on $n$$CO_2$ capture. To clarify the $n$$CO_2$-driven stabilization in the RTIL-2-propanol systems, we replotted the observed CO_2 capture against the calculated α angle (**Figure 6(b)**). The most $n$$CO_2$ capture in the [N4111]-[TFSI]-2-propanol was observed at α = 70˚. In contrast, the minimum $n$$CO_2$ capture in the [N1123]-[TFSI]-2-propanol system, which is fully stabilized without the addition of 2-propanol, was shifted to lower value of α. The α dependence of η in **Figure 6(b)** can be explained by assuming that CO_2 compensates for geometrically mismatching of $TFSI^-$ conformer and additives in 2-propanol based mixtures.

3.4. Gas Selectivity of [N4111][TFSI]-2-Propanol

For actual applications, the RTIL-propanol mixtures must be gas selective. **Figure 7** shows CO_2, O_2, and N_2 sorption in the [N4111][TFSI]-80 mol% 2-propanol system at 25˚C. N_2 cannot contribute to energetic stabilization in an unstable liquid system in the propanol-rich region. N_2 mostly occupied in the air has the lowest sorption.

Table 1. Calculated torsion angle (α) of $TFSI^-$ anion. α is strongly dependent on the presence of propanol and CO_2.

Number of molecules					
[N4111][TFSI]	Propanol	CO_2	Type of Propanol	Dipole (Debye)	α (deg)
1	0	0		15.390	30.756
1	0	1		14.983	45.338
1	1	0	1-Propanol	13.456	49.678
1	1	1	1-Propanol	13.014	36.554
1	1	0	2-Propanol	15.615	72.517
1	1	1	2-Propanol	13.589	72.736

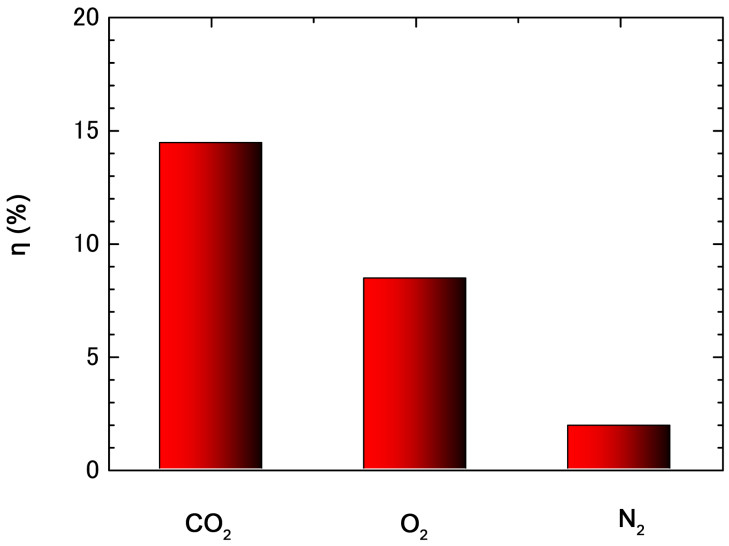

Figure 7. Gas selectivity in [N4111][TFSI]-80 mol% propanol at 25˚C.

The gas selectivity in the [N4111][TFSI]-80 mol% 2-propanol system has an advantage for industrial applications. The results clearly show that CO_2 is preferred in the [N4111][TFSI]-2-propanol system. CO_2 selectivity was realized at ambient pressure. CO_2 plays an important role for the high efficient CO_2 capture system, although the mechanism remains unclear.

4. Summary

At ambient pressure and room temperature, nCO_2 capture in quaternary ammonium-based RTILs is promoted by the addition of 2-propanol. The propanol isomer effect associated with nCO_2 capture is revealed by the lack of enhancement in RTIL with added 1-propanol. The conformation of $TFSI^-$ is regarded as a good indicator of nCO_2 capture ability, since $TFSI^-$ torsion angle is strongly correlated with the amount of nCO_2 sorption. The increase in nCO_2 sorption in the propanol-rich region is consistent with liquid instability near the UCST, as shown in the phase diagram. The [N4111][TFSI]-2-propanol mixtures provide both high nCO_2 capture and gas selectivity.

Acknowledgements

We appreciate Dr. T. Takekiyo, Dr. M. Aono and Prof. Y. Yoshimura of National Defense Academy for helpful discussions.

References

[1] Blanchard, L.A., Hancu, D., Beckman, E.J. and Brennecke, J.F. (1999) Green Processing Using Ionic Liquids and CO_2. *Nature*, **399**, 28-29. http://dx.doi.org/10.1038/19887

[2] Huang, X., Margulis, C.J., Li, Y. and Berne, B.J. (2005) Why Is the Partial Molar Volume of CO_2 So Small When Dissolved in a Room Temperature Ionic Liquid? Structure and Dynamics of CO_2 Dissolved in [$Bmim^+$] [PF_6^-]. *Journal of American Chemical Society*, **127**, 17842-17851. http://dx.doi.org/10.1021/ja055315z

[3] Zhuo, S., Huang, Y., Peng, C., Liu, H., Hu, Y. and Jiang, J. (2010) CO_2-Induced Microstructure Transition of Surfactant in Aqueous Solution: Insight from Molecular Dynamics Simulation. *Journal of Physical Chemistry B*, **114**, 6344-6349. http://dx.doi.org/10.1021/jp910253b

[4] Perez-Blanco, M.E. and Maginn, E.J. (2010) Molecular Dynamics Simulations of CO_2 at an Ionic Liquid Interface: Adsorption, Ordering, and Interfacial Crossing. *Journal of Physical Chemistry B*, **114**, 11827-11837. http://dx.doi.org/10.1021/jp103862v

[5] Babarao, R., Dai, S. and Jiang, D. (2011) Understanding the High Solubility of CO_2 in an Ionic Liquid with the Tetracyanoborate Anion. *Journal of Physical Chemistry B*, **115**, 9789-9794. http://dx.doi.org/10.1021/jp205399r

[6] Perez-Blanco, M.E. and Maginn, E.J. (2011) Molecular Dynamics Simulations of Carbon Dioxide and Water at an Ionic Liquid Interface. *Journal of Physical Chemistry B*, **115**, 10488-10499. http://dx.doi.org/10.1021/jp203838j

[7] Blanchard, L.A., Gu, Z. and Brennecke, J.F. (2001) High-Pressure Phase Behavior of Ionic Liquid/CO_2 Systems. *Journal of Physical Chemistry B*, **105**, 2437-2444. http://dx.doi.org/10.1021/jp003309d

[8] Tang, J., Tang, H., Sun, W., Plancher, H., Radosza, M. and Shen, Y. (2005) Poly(ionic liquid)s: A New Material with Enhanced and Fast CO_2 Absorption. *Chemical Communications*, 3325-3327.

[9] Sakellarios, N.I. and Kazarian, S.G. (2005) Solute Partitioning between an Ionic Liquid and High-Pressure CO_2 Studied with *in Situ* FTIR Spectroscopy. *Journal of Chemical Thermodynamics*, **37**, 621-626. http://dx.doi.org/10.1016/j.jct.2005.03.022

[10] Bara, J.E., Carlisle, T.K., Gabriel, C.J., Camper, D., Finotello, A., Gin, D.L. and Noble, R.D. (2009) Guide to CO_2 Separations in Imidazolium-Based Room-Temperature Ionic Liquids. *Industrial & Engineering Chemistry Research*, **48**, 2739-2751. http://dx.doi.org/10.1021/ie8016237

[11] Kerle, D., Ludwig, R., Geiger, A. and Paschek, D. (2009) Temperature Dependence of the Solubility of Carbon Dioxide in Imidazolium-Based Ionic Liquids. *Journal of Physical Chemistry B*, **113**, 12727-12735. http://dx.doi.org/10.1021/jp9055285

[12] Brennecke, J.F. and Gurkan, B.E. (2010) Ionic Liquids for CO_2 Capture and Emission Reduction. *Journal of Physical Chemistry Letters*, **1**, 3459-3464. http://dx.doi.org/10.1021/jz1014828

[13] Lei, Z., Han, J., Zhang, B., Li, Q., Zhu, J. and Chen, B. (2012) Solubility of CO_2 in Binary Mixtures of Room-Temperature Ionic Liquids at High Pressures. *Journal of Chemical & Engineering Data*, **57**, 2153-2159. http://dx.doi.org/10.1021/je300016q

[14] Abe, H., Mori, T., Abematsu, R., Yoshimura, Y., Hatano, N., Imai, Y. and Kishimura, H. (2012) Desorption Process in Room Temperature Ionic Liquid Based-Mixtures under Vacuum. *Journal of Molecular Liquids*, **167**, 40-46. http://dx.doi.org/10.1016/j.molliq.2011.12.009

[15] Ozawa, S., Kishimura, H., Kitahira, S., Tamatani, K., Hirayama, K., Abe, H. and Yoshimura, Y. (2014) Isomer Effect of Propanol on Liquid-Liquid Equilibrium in Hydrophobic Room-Temperature Ionic Liquids. *Chemical Physics Letters*, **613**, 122-126. http://dx.doi.org/10.1016/j.cplett.2014.09.003

[16] Abe, H., Aono, M., Kameoka, S., Tsai, A-.P., Yoshimura, Y. and Ozawa, S. (2014) Impedance Spectroscopic Study Using Nanoporous Electrode on Room Temperature Ionic Liquid-Propanol Mixtures. *Journal of Japan Institute of Energy*, **93**, 1015-1020. http://dx.doi.org/10.3775/jie.93.1015

[17] Abe, H., Fukushima, R., Onji, M., Hirayama, K., Kishimura, H., Yoshimura, Y. and Ozawa, S. (2016) Two-Length Scale Description of Hydrophobic Room-Temperature Ionic Liquid-Alcohol Systems. *Journal of Molecular Liquids*, **215**, 417-422. http://dx.doi.org/10.1016/j.molliq.2015.12.011

[18] Fujii, K., Fujimori, T., Takamuku, T., Kanzaki, R., Umebayashi, Y. and Ishiguro, S. (2006) Conformational Equilibrium of Bis(trifluoromethanesulfonyl) Imide Anion of a Room-Temperature Ionic Liquid: Raman Spectroscopic Study and DFT Calculations. *Journal of Physical Chemistry B*, **110**, 8179-8183. http://dx.doi.org/10.1021/jp0612477

[19] Fujii, K., Soejima, Y., Kyoshoin, Y., Fukuda, S., Kanzaki, R., Umebayashi, Y., Yamaguchi, T., Ishiguro, S. and Takamuku, T. (2008) Liquid Structure of Room-Temperature Ionic Liquid, 1-Ethyl-3-methylimidazolium Bis-(trifluoromethanesulfonyl) Imide. *Journal of Physical Chemistry B*, **112**, 4329-4336. http://dx.doi.org/10.1021/jp7105499

[20] Muldoon, M.J., Aki, S.N.V.K., Anderson, J.L., Dixon, J.K. and Brennecke, J.F. (2007) Improving Carbon Dioxide Solubility in Ionic Liquids. *Journal of Physical Chemistry B*, **111**, 9001-9009. http://dx.doi.org/10.1021/jp071897q

[21] Wasserscheid, P. and Welton, T. (2003) Ionic Liquids in Synthesis. Wiley, Hoboken.

[22] Lasse` gues, J.C., Grondin, J., Holomb, R. and Johansson, P. (2007) Raman and *ab initio* Study of the Conformational Isomerism in the 1-Ethyl-3-methyl-imidazolium Bis(trifluoromethanesulfonyl)imide Ionic Liquid. *Journal of Raman Spectroscopy*, **38**, 551-558. http://dx.doi.org/10.1002/jrs.1680

[23] Becke, A.D. (1993) Density-Functional Thermochemistry. III. The Role of Exact Exchange. *Journal of Chemical Physics*, **98**, 5648-5652. http://dx.doi.org/10.1063/1.464913

[24] Lee, C., Yang, W. and Parr, R.G. (1988) Development of the Colle-Salvetti Correlation-Energy Formula into a Functional of the Electron Density. *Physical Review B*, **37**, 785-789. http://dx.doi.org/10.1103/PhysRevB.37.785

[25] Schmidt, M.W., Baldridge, K.K., Boatz, .J.A., Elbert, S.T., Gordon, M.S., Jensen, J.H., Koseki, S., Matsunaga, N., Nguyen, K.A., Su, S.J., Windus, T.L., Dupuis, M. and Montgomery, J.A. (1993) General Atomic and Molecular Electronic Structure System. *Journal of Computational Chemistry*, **14**, 1347-1363. http://dx.doi.org/10.1002/jcc.540141112

[26] Yoshimura, Y., Takekiyo, T., Imai, Y. and Abe, H. (2012) Pressure-Induced Spectral Changes of Room-Temperature Ionic Liquid, *N*,*N*-Diethyl-*N*-methyl-*N*-(2-methoxyethyl)ammonium Bis(trifluoromethylsulfonyl)imide, [DEME][TFSI]. *Journal of Physical Chemistry C*, **116**, 2097-2101. http://dx.doi.org/10.1021/jp205314f

[27] Tsuzuki, S., Hayamizu, K. and Seki, S. (2010) Origin of the Low-Viscosity of [emim][$(FSO_2)_2N$] Ionic Liquid and Its Lithium Salt Mixture: Experimental and Theoretical Study of Self-Diffusion Coefficients, Conductivities, and Intermolecular Interactions. *Journal of Physical Chemistry B*, **114**, 16329-16336. http://dx.doi.org/10.1021/jp106870v